Supporting material

Modification of Thermally Activated Delayed Fluorescence Emitters Comprising Fluorinated Acridan-Quinazoline or Spiroacridan Moieties for Efficient Green OLEDs

Fu-En Szu[a], Shao-An Chen[b], Yin-Yin Yu[a], Jiun-Haw Lee[b]*, Tien-Lung Chiu[c]* and Man-kit Leung[a,d]*

[a] *Department of Chemistry, National Taiwan University, Taipei 10617, Taiwan.*

[b] *Graduate Institute of Photonics and Optoelectronics and Department of Electrical Engineering, National Taiwan University, Taipei 10617, Taiwan.*

[c] *Department of Electrical Engineering, Yuan Ze University, Chung-Li, Taoyuan 32003, Taiwan.*

[d] *Advanced Research Center for Green Materials Science and Technology, National Taiwan University No. 1, Sec. 4, Roosevelt Rd., Taipei 10617, Taiwan (R.O.C.)*

Email : jiunhawlee@ntu.edu.tw; tlchiu@saturn.yzu.edu.tw; mkleung@ntu.edu.tw;

Experimental Section

10,10'-((5-fluoroquinazoline-2,4-diyl)bis(4,1-phenylene))bis(9,9-dimethyl-9,10-dihydroacridine)

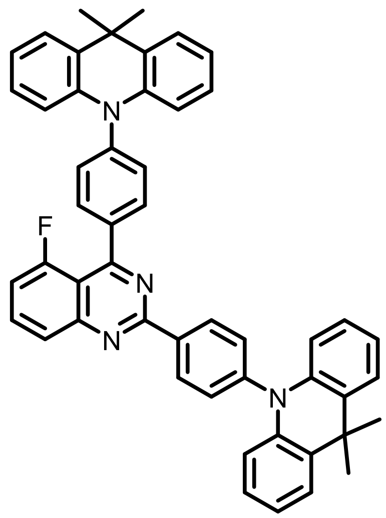

4Ac5FQN

A two-neck flask under argon atmosphere was charged with $Pd_2(dba)_3$ (229 mg, 0.1 mmol), 5-Fluoro-2,4-bis(4-bromophenyl)quinazoline (458 mg, 1.0 mmol), sodium tert-butoxide (721 mg, 3.0 mmol), XPhos (238 mg, 0.2 mmol) and 9,9-dimethyl-9,10-dihydroacridine (2.2 mmol). Dry and de-aerated toluene (10 mL) was added. The mixture was refluxed for 15 h. After cooling, the reaction mixture was diluted with dichloromethane and filtered through celite, then dried over anhydrous $MgSO_4$. The solvent was evaporated by vacuum and the crude product was purified by column chromatography on silica gel (DCM/Hexane = 1/3). ^{1}H NMR (400 MHz, Chloroform-d_1): δ 8.94 (d, J = 8.4 Hz, 2 H), δ 8.08-8.03 (m, 3 H), δ 7.95-7.89 (m, 1 H), δ 7.53 (dd, J = 8.4 Hz, 3.8 Hz, 5 H), δ 7.49-7.15 (m, 4 H), δ 7.33-7.28 (m, 1 H), δ 7.05-7.00 (m, 3 H), δ 6.98-6.91 (m, 6 H), δ 6.44 (d, J = 8.2 Hz, 2 H), δ 6.37 (d, J = 8.2 Hz, 2 H), δ 1.71 (s, 12 H); ^{13}C NMR (100 MHz, Chloroform-d_1): δ 167.07, 165.67, 159.89, 159.25, 156.65, 153.47, 143.89, 142.75, 140.77, 140.69, 139.79, 137.43, 134.49, 134.23, 134.14, 131.98, 131.93, 131.64, 131.45, 130.82, 130.18, 130.07, 126.46, 126.39, 125.63, 125.30, 125.25, 120.77, 120.69, 114.22, 114.14, 112.90, 112.82, 112.70, 36.06, 36.01, 31.35, 31.20; HRMS calcd. for $C_{50}H_{40}FN_4$ ($M+1^+$) 715.3237, obsd. 715.3232

Figure S1. [1]H NMR spectrum of **4Ac5FQN**.

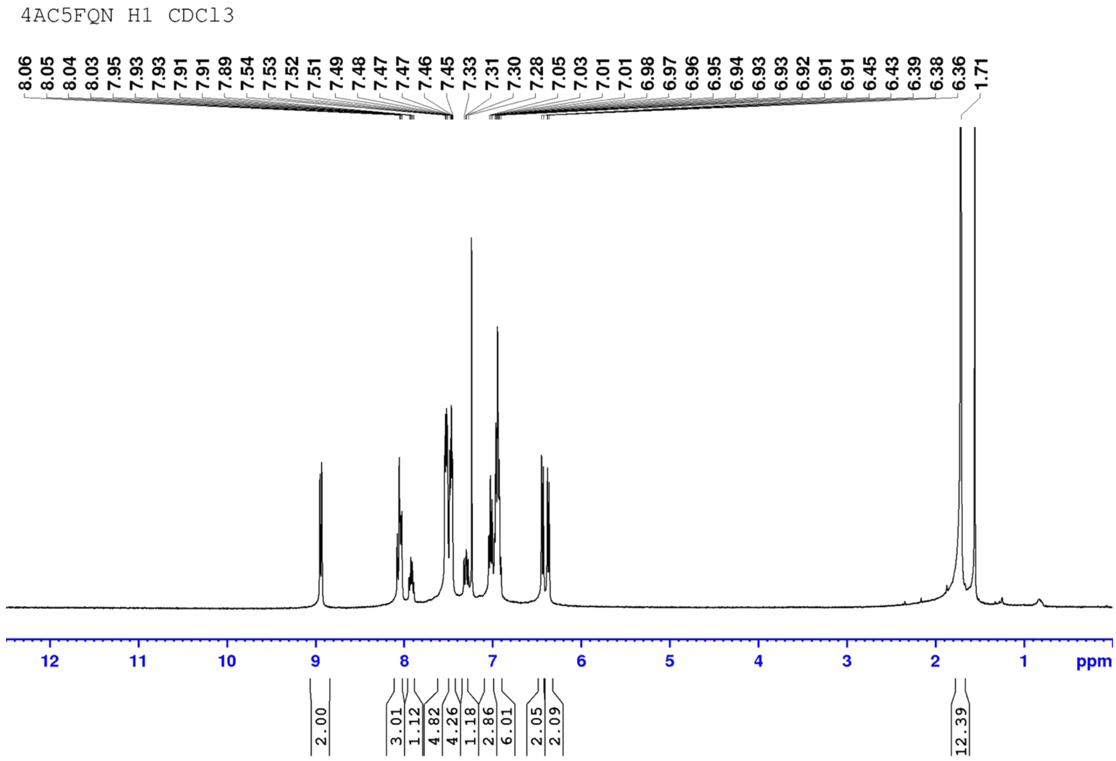

Figure S2. [13]C NMR spectrum of compound **4Ac5FQN**.

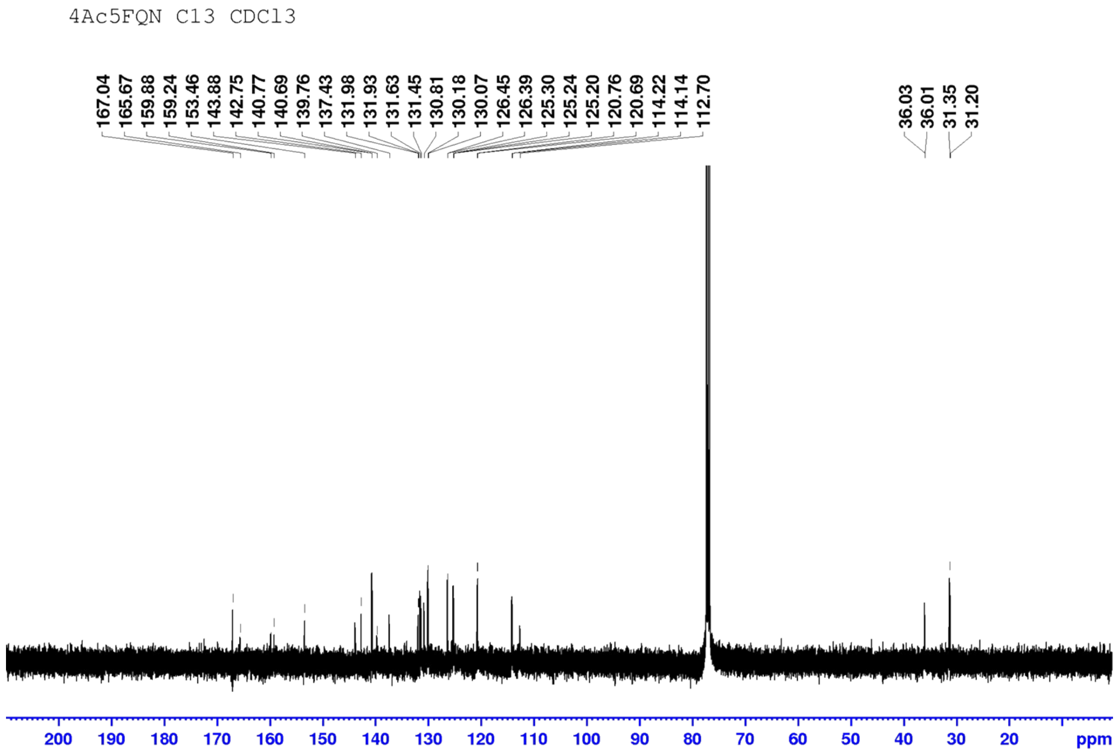

Figure S3. ^{19}F NMR spectrum of compound **4Ac5FQN**.

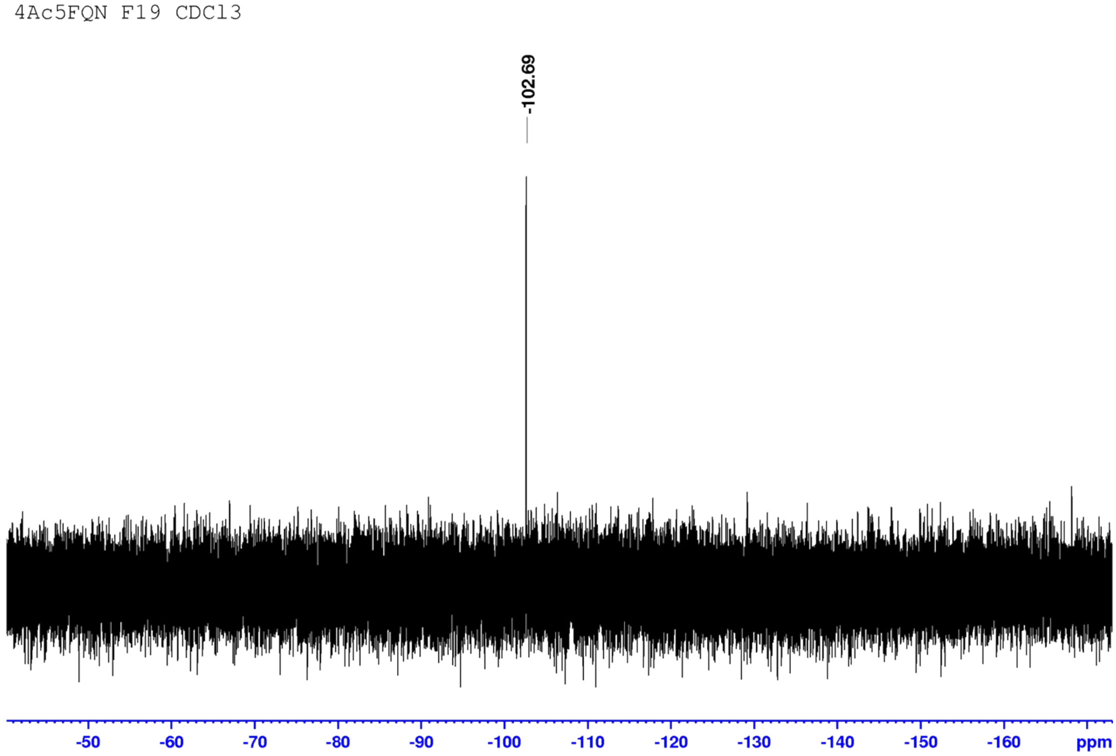

10,10''-((5-fluoroquinazoline-2,4-diyl)bis(4,1-phenylene))bis(10H-spiro[acridine-9,9'-fluorene])

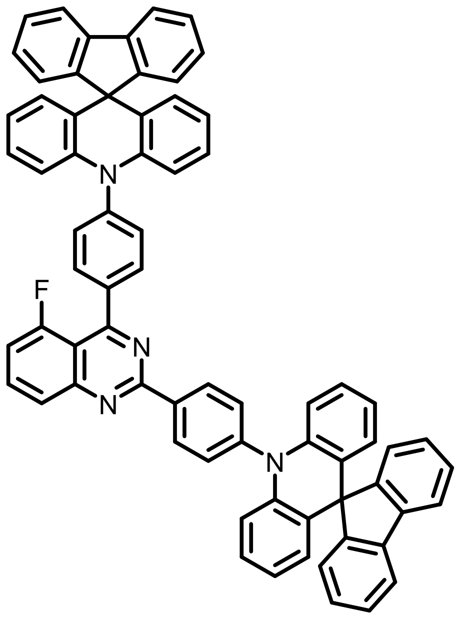

4SpAc5FQN

A two-neck flask under argon atmosphere was charged with $Pd_2(dba)_3$ (229 mg, 0.1 mmol), 5-fluoro-2,4-bis(4-bromophenyl)quinazoline (458 mg, 1.0 mmol), sodium tert-butoxide (721 mg, 3.0 mmol), XPhos (238mg, 0.2mmol) and 10H-spiro[acridine-9,9'-fluorene] (2.2 mmol). Dry and de-aerated toluene (10 mL) was added. The mixture was refluxed for 15 h. After cooling, the reaction mixture was diluted with dichloromethane and filtered through celite, then dried over anhydrous $MgSO_4$. The solvent was evaporated by vacuum and the crude product was purified by column chromatography on silica gel (DCM/Hexane = 1/3). ^1H NMR (400 MHz, Chloroform-d_1): δ 9.05 (d, J = 8.4 Hz, 2H), 8.16~8.11 (m, 3H), 7.98~7.94 (m, 1H), 7.80 (dd, J = 7.7 Hz, 2.6 Hz, 4H), 7.70 (d, J = 8.4 Hz, 4 H), 7.46 (dd, J = 7.5 Hz, 2.6 Hz, 4H), 7.39~7.32 (m, 5H), 7.27 (d, J = 7.4 Hz, 4H), 6.98 (td, J = 7.6 Hz, 1.3 Hz, 2H), 6.92 (td, J = 7.6 Hz, 1.3 Hz, 2H), 6.62~6.53 (m, 6H), 6.49~6.41 (m, 6H); ^{13}C NMR (100 MHz, Chloroform-d_1): δ 159.87, 156.57, 156.51, 153.51, 143.75, 142.62, 141.15, 141.09, 132.18, 131.67, 131.63, 130.85, 128.39, 127.85, 127.61, 127.25, 125.79, 124.96, 124.88, 120.79, 120.72, 119.91, 119.89, 114.73, 114.68, 56.82; HRMS calcd. for $C_{70}H_{44}FN_4$ ($M+1^+$) 959.3550, obsd. 959.3543

Figure S4. ^{1}H NMR spectrum of **4SpAc5FQN**.

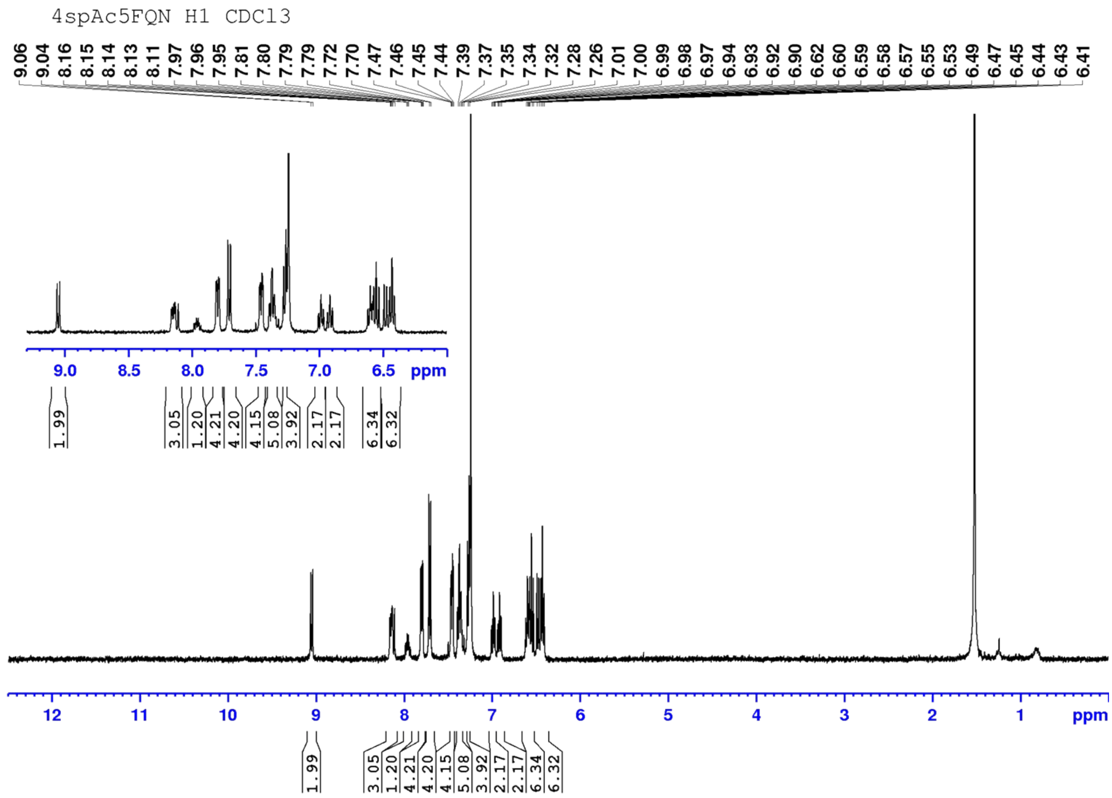

Figure S5. ^{13}C NMR spectrum of compound **4SpAc5FQN**.

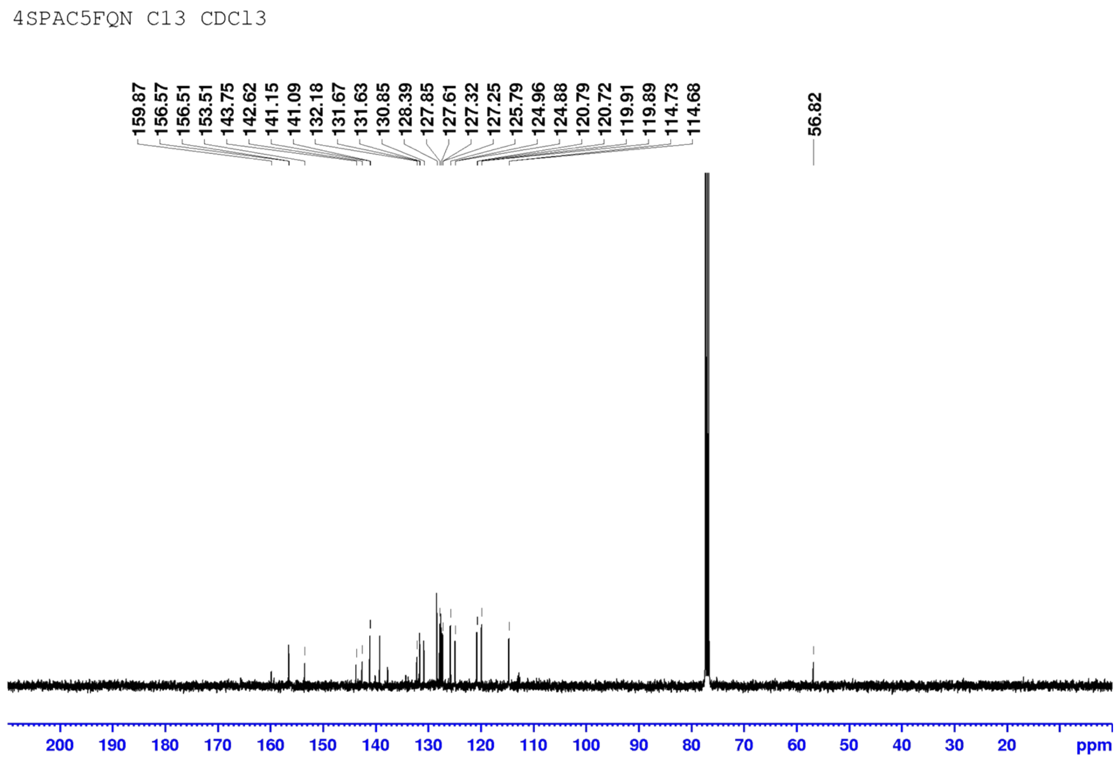

Figure S6. ^{19}F NMR spectrum of compound **4SpAc5FQN**.

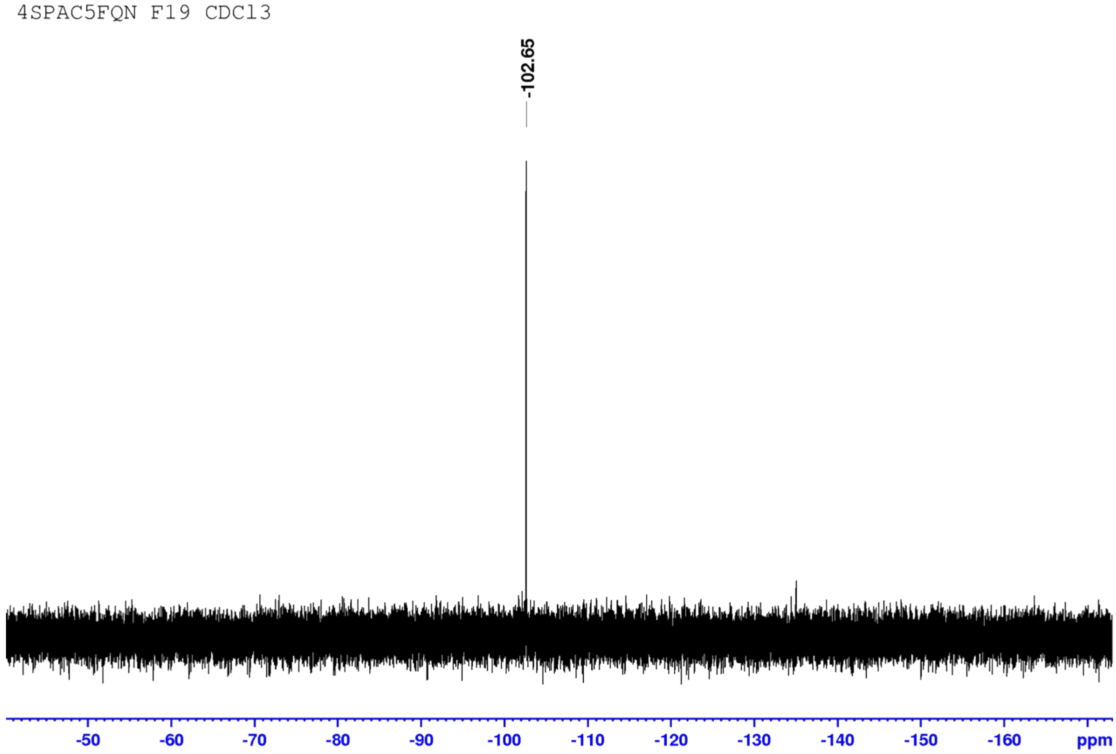

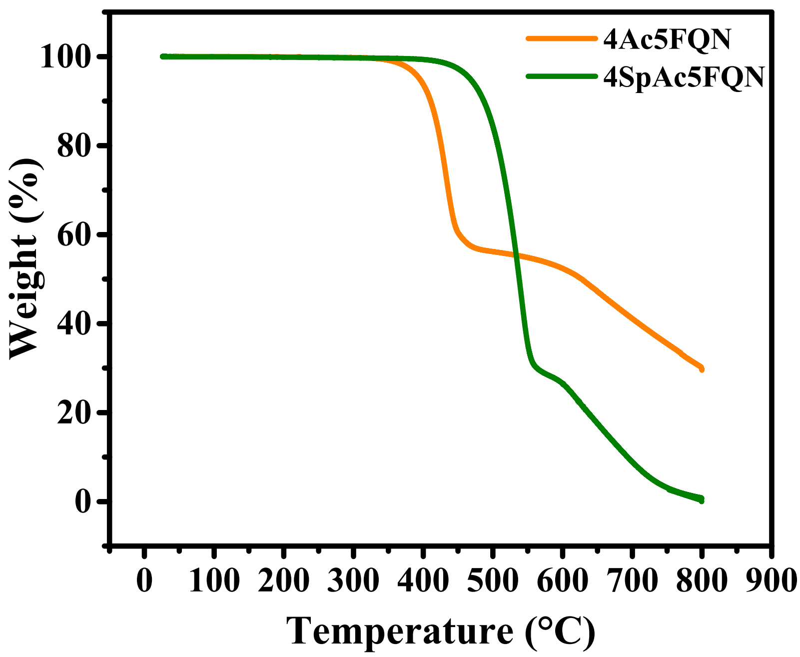

Figure S7. Thermal gravity analysis (TGA) curves of **4Ac5FQN** and **4SpAc5FQN**.

(a)

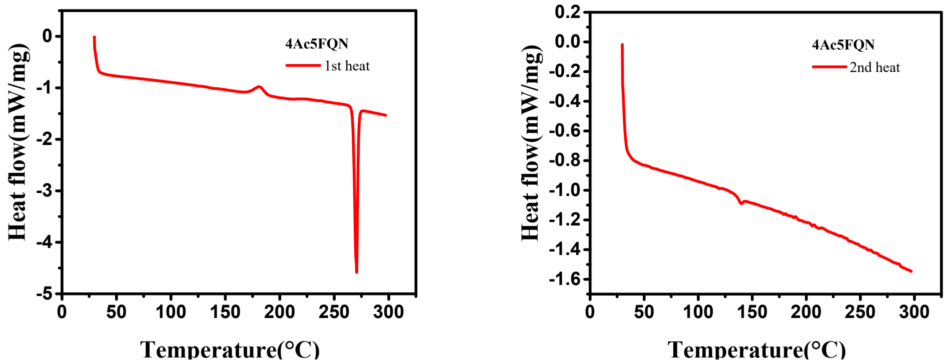

(b)

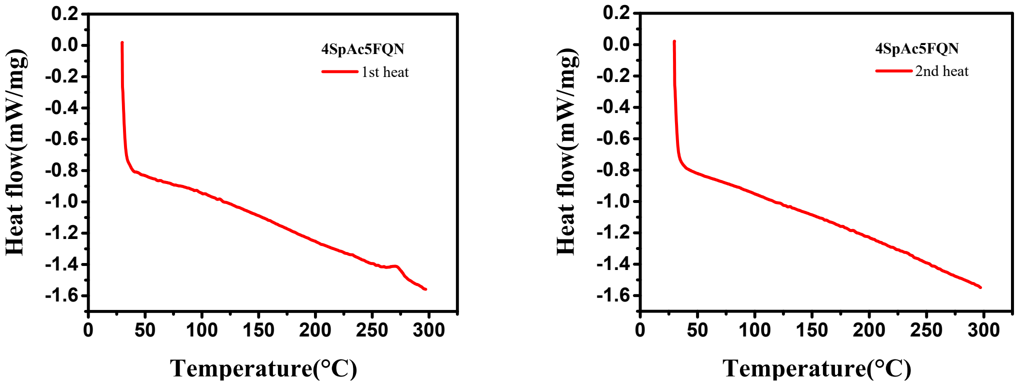

Figure S8. Differential scanning calorimetry (DSC) curves of (a) **4Ac5FQN** and (b) **4SpAc5FQN**.

(a)

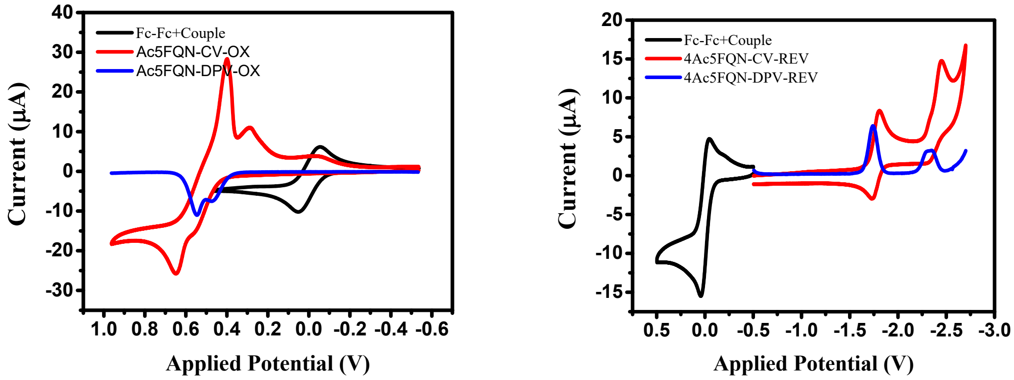

(b)

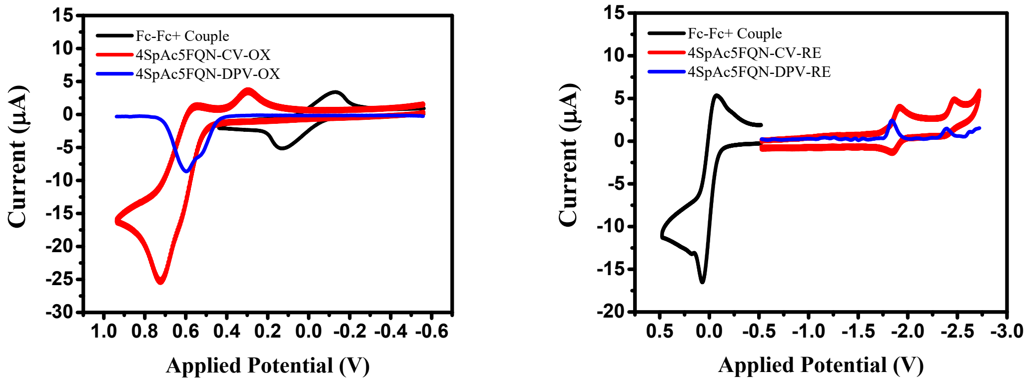

Figure S9. Cyclic voltammogram (CV) and differential pulse voltammetry (DPV) of (a) **4Ac5FQN** and (b) **4SpAc5FQN**.

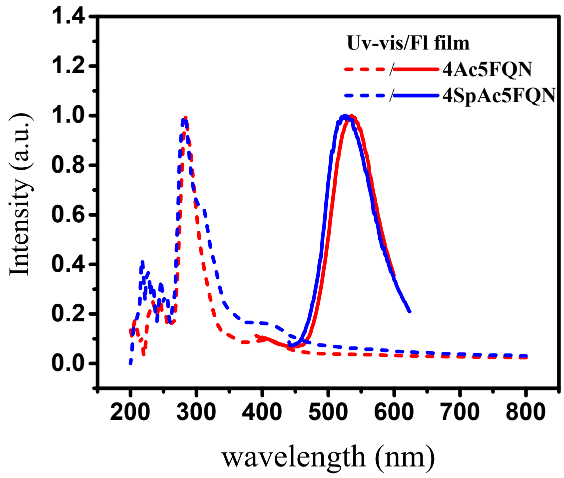

Figure S10. PL of thin film with **4Ac5FQN** and **4SpAc5FQN**

Table S1. Device structure of OLEDs with **4Ac5FQN** as emitter.

Device	**HTL** **TAPC**	**EBL** **mCP**	**EML** ***o*-DiCbzBz/X%** **4Ac5FQN**	**ETL** **DPPS**	**cathode** **LiF/Al**
A-1			30/5%		
A-2			30/10%	45	
A-3			30/15%		
A-4	50	10			1/120
A-5				50	
A-6			30/5%	55	
A-7				60	
A-8				65	
Unit:nm					

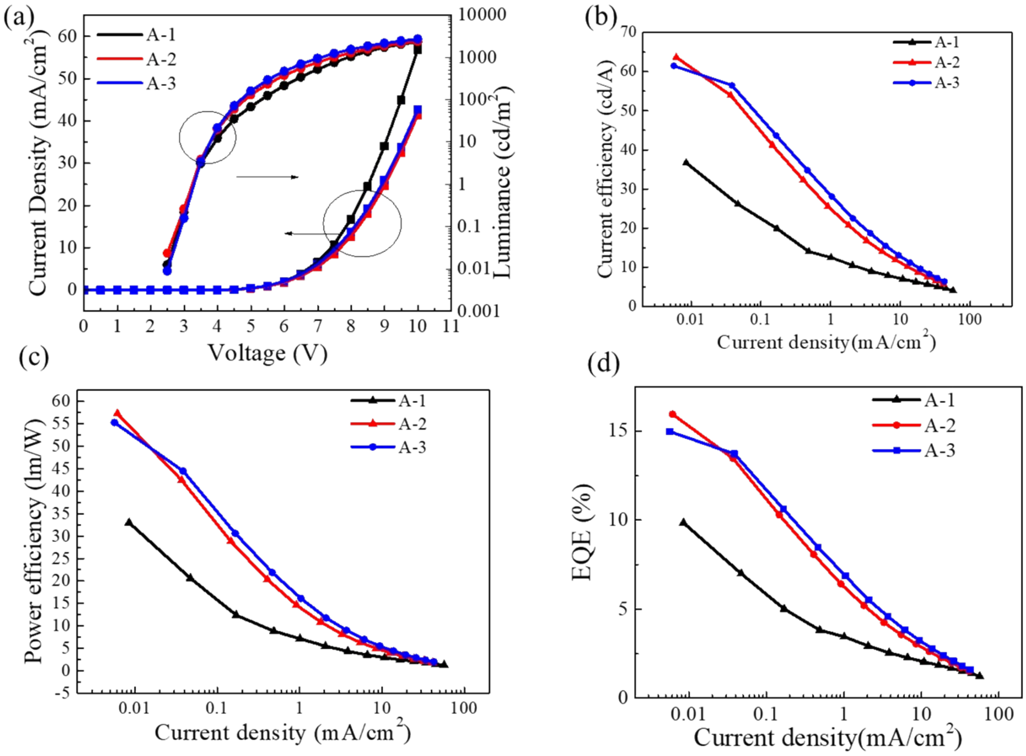

Figure S11. Device performance of (a) J-L-V; (b)CE-J; (c)PE-J; (d) EQE-J for OLEDs (A-1, A-2, A-3)

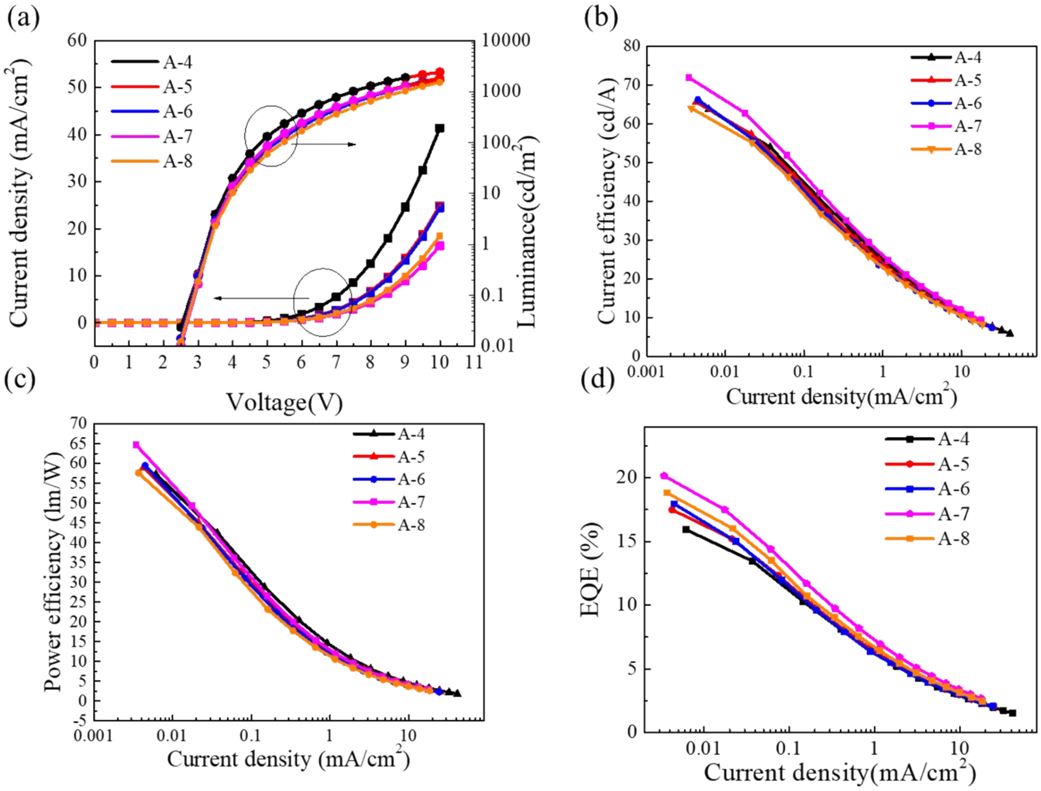

Figure S12. Device performance of (a) J-L-V; (b)CE-J; (c)PE-J; (d) EQE-J for OLEDs (A-4, A-5, A-6, A-7, A-8)

Table S2. Device performance of OLEDs with **4Ac5FQN** as emitter.

Device	EML/ETL (%, nm)	Voltage [a] (V)	Luminance [b] (cd/m^2)	CE [c] (cd/A)	PE [c] (lm/W)	EQE [c] (%)	CIE [d] (x,y)
A-1	1%, 30/45	7.39	2290	36.70/12.94/6.54	33.01/7.71/2.47	9.84/3.61/1.86	(0.257,0.515)
A-2	**5%, 30/45**	**7.66**	**2406**	**63.67/34.30/12.03**	**57.28/22.23/5.02**	**15.94/8.59/3.05**	**(0.327,0.581)**
A-3	10%, 30/45	7.55	2710	61.50/38.87/14.98	55.30/25.76/6.71	14.97/9.42/3.72	(0.347,0.585)
A-4	5%, 30/45	7.66	2406	66.52/34.64/11.94	59.86/22.55/5.02	15.94/8.67/3.05	(0.327,0.581)
A-5	5%, 30/50	8.51	1841	70.86/33.14/11.33	63.73/19.93/4.28	17.48/8.80/3.08	(0.323,0.582)
A-6	5%, 30/55	8.56	1797	72.39/31.57/10.86	65.70/18.78/4.03	17.96/8.50/3.00	(0.328,0.581)
A-7	**5%, 30/60**	**9.00**	**1666**	**71.90/40.51/14.45**	**64.73/29.31/7.14**	**20.15/11.28/4.10**	**(0.351,0.578)**
A-8	5%, 30/65	9.00	1513	75.70/31.44/10.59	68.08/18.15/3.74	18.83/9.14/3.17	(0.351,0.576)

[a] at J= 10mA/cm^2; [b] Maximum; [c] CE/PE/EQE measured at maximum/100 cd/m^2/1000 cd/m^2; [d] at 4 V.

Table S3. Device structure of OLEDs with **4SpAc5FQN** as emitter.

Device	HTL TAPC	EBL mCP	EML *o*-DiCbzBz/X% 4SpAc5FQN	ETL DPPS	cathode LiF/Al
A-1	50	10	30/5%	45	1/120
A-2			30/10%		
A-3			30/15%		
A-4			30/20%		
A-5			30/15%		
A-6				50	
A-7				55	
A-8				60	
Unit:nm					

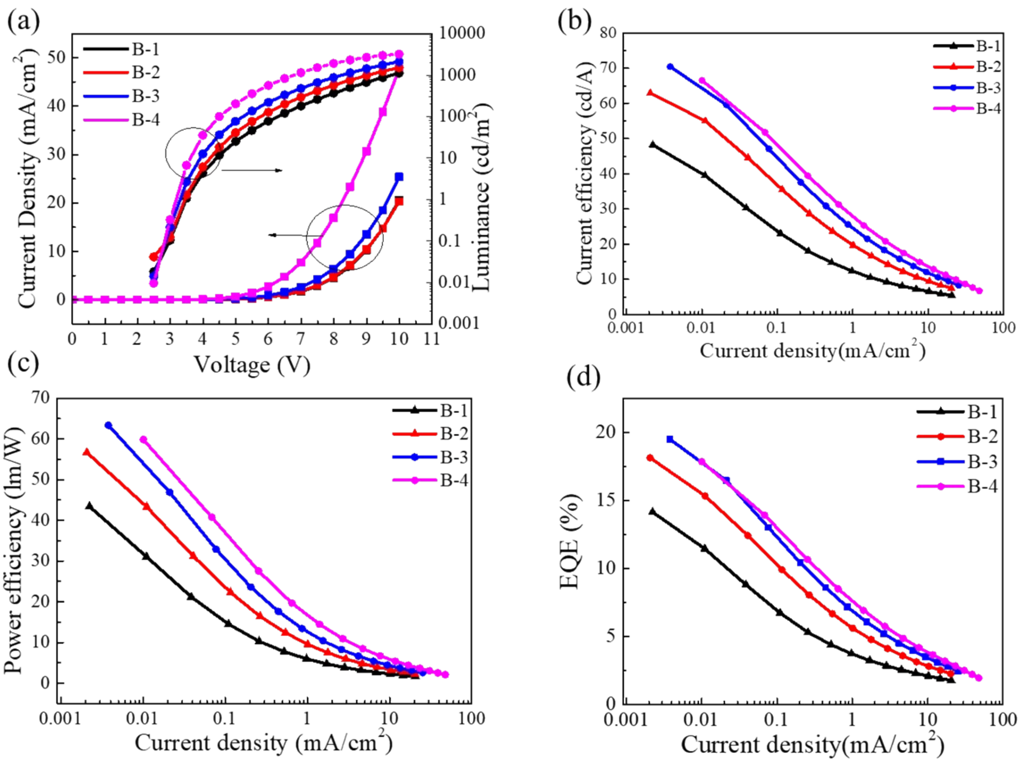

Figure S13. Device performance of (a) J-L-V; (b)CE-J; (c)PE-J; (d) EQE-J for OLEDs (B-1, B-2, B-3, B-4)

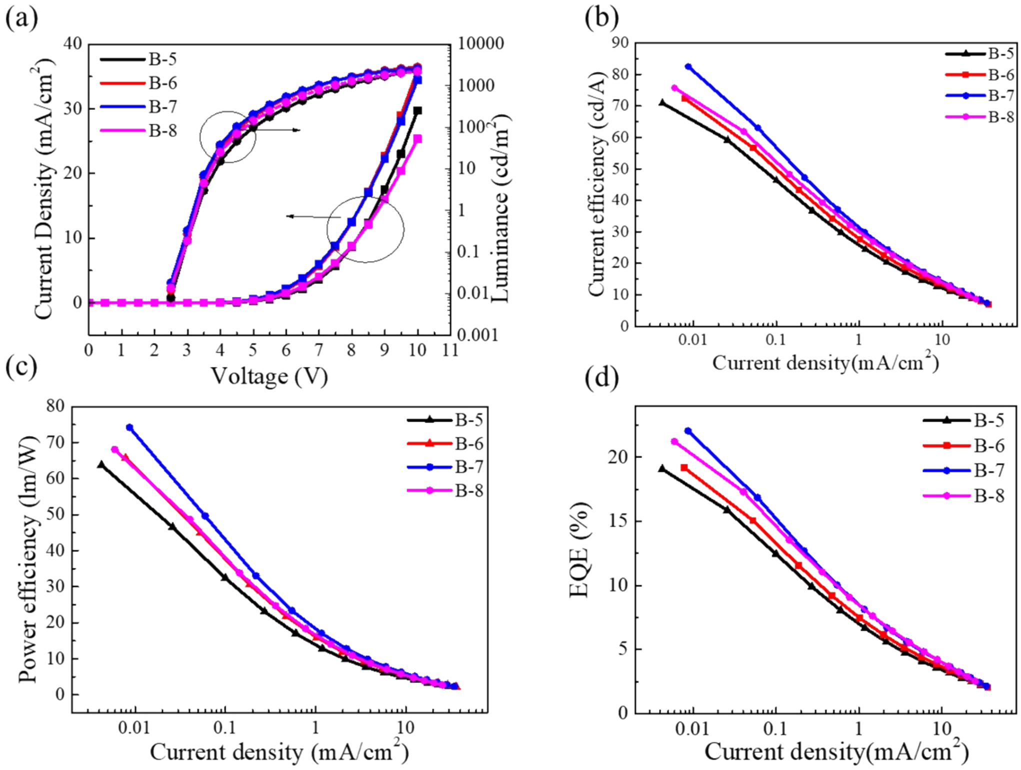

Figure S14. Device performance of (a) J-L-V; (b)CE-J; (c)PE-J; (d) EQE-J for OLEDs (B-5, B-6, B-7 , B-8)

Table S4. Device performance of OLEDs with **4SpAc5FQN** as emitter.

Device	EML/ETL (%, nm)	Voltage [a] (V)	Luminance [b] (cd/m^2)	CE [c] (cd/A)	PE [c] (lm/W)	EQE [c] (%)	CIE [d] (x,y)
B-1	5%, 30/45	8.95	1115	48.24/13.15/5.66	43.40/6.53/1.82	14.14/3.93/1.82	(0.274,0.535)
B-2	10%, 30/45	8.93	1519	62.96/25.73/9.30	56.68/14.08/3.24	18.13/7.27/2.77	(0.317,0.565)
B-3	**15%, 30/45**	**8.56**	**2106**	**70.46/33.47/12.92**	**63.37/19.91/4.90**	**19.50/9.30/3.72**	**(0.327,0.577)**
B-4	20%, 30/45	7.28	3203	66.52/39.90/15.90	59.86/28.13/7.36	17.85/10.81/4.42	(0.335,0.576)
B-5	15%, 30/45	8.16	2292	70.86/37.85/13.37	63.73/24.30/5.40	19.07/10.21/3.74	(0.328,0.577)
B-6	15%, 30/50	7.67	2800	72.39/40.90/15.95	65.70/28.20/7.23	19.18/10.94/4.42	(0.336,0.575)
B-7	**15%, 30/55**	**7.64**	**2570**	**82.50/47.80/17.54**	**74.19/33.56/7.94**	**22.06/12.84/4.86**	**(0.348,0.580)**
B-8	15%, 30/60	8.16	2197	75.70/44.61/16.99	68.08/31.64/7.16	21.23/12.04/4.88	(0.369,0.572)

[a] at J= $10mA/cm^2$; [b] Maximum; [c] CE/PE/EQE measured at maximum/100 cd/m^2/1000 cd/m^2; [d] at 4 V.

(a) 4Ac5FQN

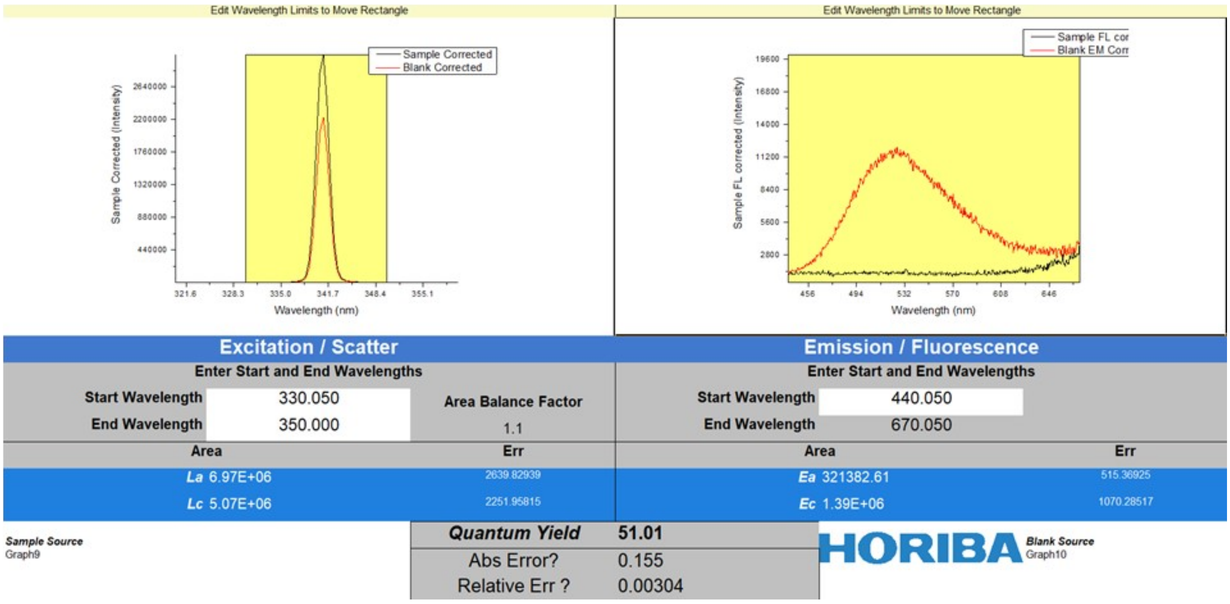

(b) 4SpAc5FQN

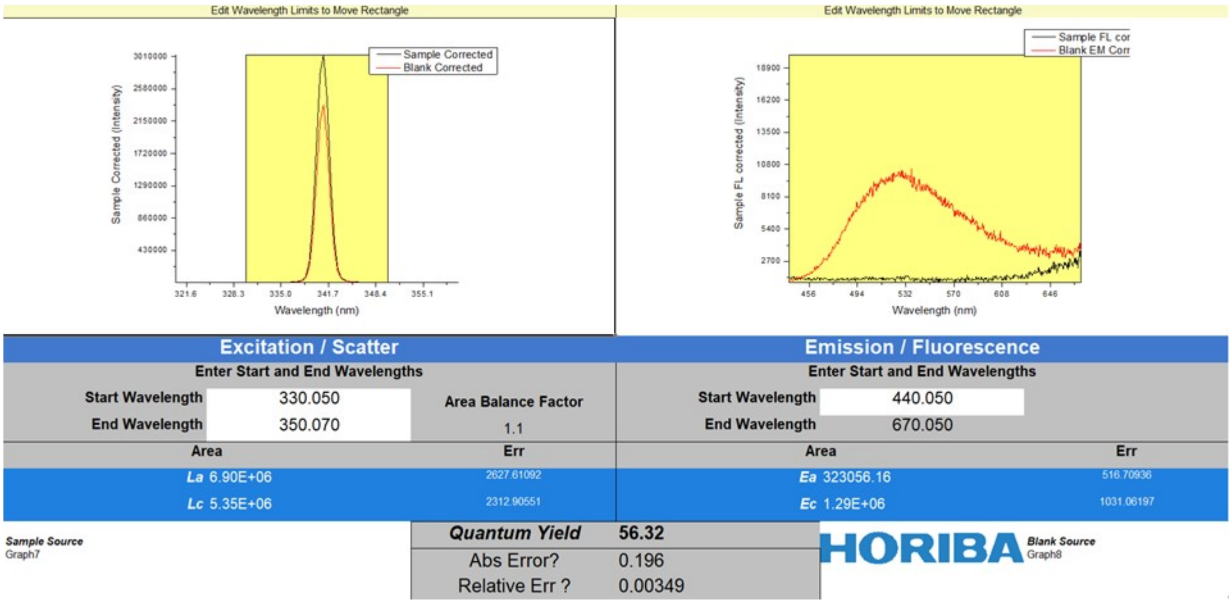

Figure S15. PLQY of mixed film (a) **4Ac5FQN** doped *o*-DiCbzBZ; (b) **4SpAc5FQN** doped *o*-DiCbzBZ.

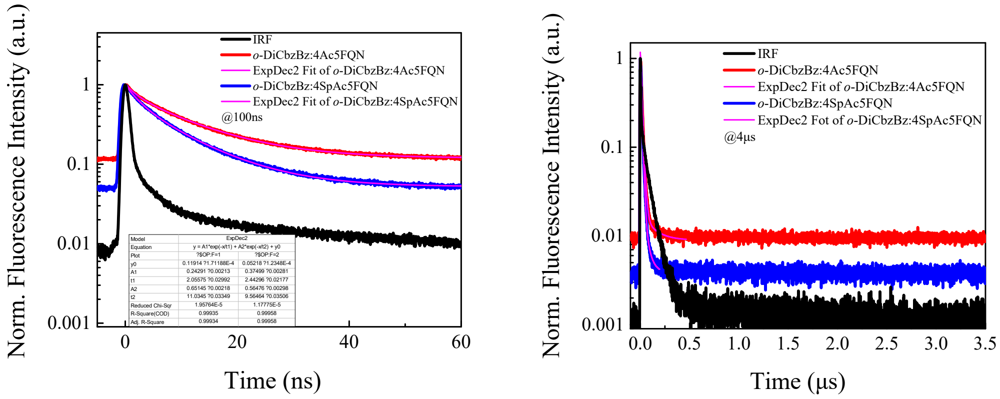

Figure S16. TrPL of prompt and delayed decay curves for **4Ac5FQN** and **4SpAc5FQN** in doped film.